Naval Surface Warfare Center
Carderock Division
West Bethesda, MD 20817-5700

NSWCCD-50-TR–2007/079 November 2007

Hydromechanics Department Report

A New Approach to Satisfy Dynamic Similarity for Model Submarine Maneuvers

by

Young T. Shen and David E. Hess

NSWCCD-50-TR–2007/079 A New Approach to Satisfy Dynamic Similarity for Model Submarine Maneuvers

THIS PAGE INTENTIONALLY LEFT BLANK

REPORT DOCUMENTATION PAGE

Form Approved
OMB No. 0704-0188

1. REPORT DATE *(DD-MM-YYYY)*	2. REPORT TYPE	3. DATES COVERED *(From - To)*
28-Nov-2007	Final	1 Oct 2006 - 31 Dec 2007

4. TITLE AND SUBTITLE

A New Approach to Satisfy Dynamic Similarity for Model Submarine Maneuvers

5a. CONTRACT NUMBER
N00014-07-WX-2-0502

5b. GRANT NUMBER

5c. PROGRAM ELEMENT NUMBER
0601153N

6. AUTHOR(S)

Young T. Shen and David E. Hess

5d. PROJECT NUMBER

5e. TASK NUMBER

5f. WORK UNIT NUMBER
07-1-5600-150-10

7. PERFORMING ORGANIZATION NAME(S) AND ADDRESS(ES) AND ADDRESS(ES)

Naval Surface Warfare Center
Carderock Division
9500 MacArthur Boulevard
West Bethesda, MD 20817-5700

Young T. Shen, Code 5400
David E. Hess, Code 5600

8. PERFORMING ORGANIZATION REPORT NUMBER

NSWCCD-50-TR-2007/079

9. SPONSORING / MONITORING AGENCY NAME(S) AND ADDRESS(ES)

Attn: Dr. Ronald D. Joslin, Code 331
Chief of Naval Research
One Liberty Center
875 North Randolph St
Arlington, VA 22203-5700

10. SPONSOR/MONITOR'S ACRONYM(S)
ONR

11. SPONSOR/MONITOR'S REPORT NUMBER(S)

12. DISTRIBUTION / AVAILABILITY STATEMENT

Approved for public release: distribution unlimited.

13. SUPPLEMENTARY NOTES

14. ABSTRACT

Dimensional analysis and dynamic similarity requirements show that Reynolds, Froude, and Strouhal scales are important parameters to be satisfied for free-running submarine model maneuvering tests in order that they correctly represent full scale behavior. The requirement that all three scales be satisfied simultaneously presents conflicting demands on the relationship between the velocity U and the characteristic length L of the model. The inability to meet these demands presents technical challenges to properly satisfy dynamic similarity for Radio-Controlled Model (RCM) maneuvering tests. Instead, we take a first principles approach by considering the forces and moments acting on the vehicle and seek solutions that dynamically produce the same scaled forces and moments on the model as exist on the full scale vehicle. In this manner we dynamically satisfy the above three scaling parameters. The completion of the theory will lead to the development of a modified test procedure for and subsequent validation by free-running submarine model maneuvering experiments.

Summarizing, we will develop an extended dynamic similarity theory that can be applied to the unsteady maneuvers of the RCM. We will apply the theory practically to improve the RCM test program and increase correlation with full scale data. This will provide a physical basis for deciding which improvements are better made in simulation and also enhance the model the model simulation paradigm.

15. SUBJECT TERMS

scaling model submarine maneuvers, dynamic similarity, dimensional analysis

16. SECURITY CLASSIFICATION OF:			17. LIMITATION OF ABSTRACT	18. NUMBER OF PAGES	19a. NAME OF RESPONSIBLE PERSON
a. REPORT	b. ABSTRACT	c. THIS PAGE			Young T. Shen
UNCLASSIFIED	UNCLASSIFIED	UNCLASSIFIED	UL	40	19b. TELEPHONE NUMBER *(include area code)* 301-227-1411

THIS PAGE INTENTIONALLY LEFT BLANK

Contents

Figures

Page

Tables

Page

THIS PAGE INTENTIONALLY LEFT BLANK

Abstract

Dimensional analysis and dynamic similarity requirements show that Reynolds, Froude, and Strouhal scales are important parameters to be satisfied for free-running submarine model maneuvering tests in order that they correctly represent full scale behavior. The requirement that all three scales be satisfied simultaneously presents conflicting demands on the relationship between the velocity U and the characteristic length L of the model. The inability to meet these demands presents technical challenges to properly satisfy dynamic similarity for Radio-Controlled Model (RCM) maneuvering tests. Instead, we take a first principles approach by considering the forces and moments acting on the vehicle and seek solutions that dynamically produce the same scaled forces and moments on the model as exist on the full scale vehicle. In this manner we dynamically satisfy the above three scaling parameters. The completion of the theory will lead to the development of a modified test procedure for and subsequent validation by free-running submarine model maneuvering experiments.

Summarizing, we will develop an extended dynamic similarity theory that can be applied to the unsteady maneuvers of the RCM. We will apply the theory practically to improve the RCM test program and increase correlation with full scale data. This will provide a physical basis for deciding which improvements are better made in simulation and also enhance the *model the model* simulation paradigm.

Administrative Information

The work described in this report was performed by the Propulsion and Fluid Systems Division (Code 5400) and the Maneuvering and Control Division (Code 5600) of the Hydromechanics Department at the Naval Surface Warfare Center, Carderock Division (NSWCCD). The work was funded by the Office of Naval Research, Code 331 as part of the Scaling Task of the FY07 6.1 Turbulence and Stratified Wakes Program (Program Element 0601153N).

Introduction

The Radio-Controlled Model (RCM) is a semi-autonomous, battery-powered, free-running $1/16^{th}$ to $1/20^{th}$-scale submarine model that can be configured as a model of any of the submarine classes in the fleet. Because it is free running, it can move in all six degrees of freedom and provide an unsteady maneuvering capability. The RCM can perform a wide range of maneuvers and is currently the best predictor of full-scale submarine maneuvering performance. It is an integral part of the hydrodynamic process employed by the Maneuvering and Control Division to develop Submerged Operating Envelopes and other hydrodynamic products (Hess et al, 2004).

When RCM maneuvering simulation data are compared with full-scale data, they exhibit varying degrees of Reynolds scale effect. Forces and moments acting on the ship hull, appendages and on the propulsor are known to experience such scale effects. With a two-order-of-magnitude difference in Reynolds number between model and full scale, one should not be surprised to see scale effects appearing in such typical RCM maneuvers as: turns, rudder jam recoveries and sternplane jam recoveries.

To see how the Froude scale arises, consider a deeply submerged submarine undergoing a maneuver which results in pitching (and/or rolling) motion. The initial phase of the ship motion response is characterized by the excitation moment and countered by the restoring moment. The latter is a product of ship weight and a moment arm produced by the sine component of metacentric height. The submarine pitch equation of motion, when made dimensionless, gives rise to a dimensionless quantity, which represents the ratio of the hydrodynamic exciting moment to the hydrostatic restoring moment. This quantity is identical to the Froude number as it expresses the ratio of inertial to gravitational effects acting on the submarine. To simulate the restoring moment correctly in model tests, Froude scaling must be used, and this dictates the model approach speed (Hess et al, 2004).

As a free running model, the RCM exhibits unsteady motion during maneuvering simulations. Theodorsen (1935) shows that the unsteady dynamic lift and phase on a sinusoidal pitching foil oscillatory motion are uniquely characterized by the reduced frequency. For RCM maneuvers, the ship motion is not solely oscillatory; instead, the phase and unsteady load acting on the RCM model in unsteady maneuvering are characterized by the Strouhal number (Schlichting, 1979 and Blake, 1984). Strouhal scaling is therefore important for RCM maneuvering simulation.

In addition to the Strouhal scale, RCM data clearly show that both Froude (Fr) and Reynolds scales (Re) are needed to satisfy the dynamic similarity requirement, yet this cannot be accomplished when fresh water is used for model testing. Fluid material parameters such as density, ρ, dynamic viscosity, μ, and hence kinematic viscosity, ν, are quite similar for salt water and fresh water. Therefore, when matching Reynolds and Froude numbers at both scales, one must chiefly rely on the variation in length and velocity scales because the fluid material parameters are nearly the same. Once the length scale is set by the chosen model scale ratio, then the velocity scale is used to effect the matching. When Froude scaling is applied to set the test speed, one finds that the Reynolds number is 80 to 100 times greater at full scale than at model scale. Consequently, the boundary layer thickness and boundary layer velocity profile are quite different between full scale and model scale. This explains the unavoidable appearance of Reynolds scale effects in RCM data.

Extensive test programs were carried out in the 1980's and 1990's to improve RCM simulation test results. One area of difficulty, RCM casualty recovery simulation, showed insufficient craft pitch-up motion when compared with full-scale data. A method to enhance pitch was found, and it involved the application of a layer of heavy grit on the upper surface of the hull. Furthermore, the grit appeared to have no untoward effect for maneuvers where it was not normally required. This grit method has been used since the 1990's for all RCM maneuvering simulation tests.

Over the years, however, RCM data with grit has displayed mixed results with good correlation in some tests and poor correlation in others. The mixed results with grit and the fundamental fact that Reynolds numbers cannot be matched led to the conclusion that the test program should be augmented with fixes applied in simulation. This *model the model* approach remains the current standard to ensure the reliability and accuracy of the existing RCM test method to simulate full-scale performance.

While the RCM remains the best predictor of full-scale submarine maneuvering performance, we believe that improvements to the test program can be made, which will then

have a favorable impact for modeling. This is not an easy task. Clearly, the flow field around the vehicle is quite complex during maneuvering and particularly during casualty recovery, and a reliable numerical model requires extensive correlation and verification with model and full-scale data. We observe the following fundamental issues associated with the existing RCM test method.

- The physics associated with the use of a grit layer to improve maneuvering is not understood.
- Froude scaling is currently used to set the model approach speed. For unsteady maneuvering, the requirement should be that the Froude number is matched at each instant of time throughout the maneuver. The implication is that the ratio of the hydrodynamic exciting moment to the hydrostatic restoring moment may not remain correct throughout the maneuver.
- Reynolds scale effects cause forces and moments induced by full scale appendages and the hull to be inadequately simulated in RCM tests.
- Strouhal scale which is an important parameter influencing unsteady motions is not considered in RCM tests.
- Existing scaling formulas that relate model data to full scale performance are not rigorously derived.

The interrelated consequences of each of these issues for the maneuvering model are not understood. Some of the impacts may well be mitigated, whereas others may be amplified. This is a fundamental question that needs to be kept in mind. As the theory unfolds in the Technical Approach section, the challenge will be to apply it in a practical manner to improve not only RCM maneuvers, but also the resulting model the model simulation process.

Objectives

Develop an extended dynamic similarity theory that can be applied to the unsteady maneuvers of the RCM. Apply the theory practically to improve the RCM test program and increase correlation with full scale data. Provide a physical basis for improvements that are better made in simulation and enhance the model the model simulation process.

Technical Approach

Dimensional analysis and dynamic similarity requirements show that Reynolds, Froude, and Strouhal scales must be preserved in RCM maneuvering simulation tests (Baker, 1973; Gukhman, 1965). Let Re denote the Reynolds number, which is defined by $Re = UL/\nu$, where U and L denote a characteristic speed and length, respectively. Define Fr as the Froude number given by $Fr = U/\sqrt{gL}$. Finally, St denotes the Strouhal number represented by $St = (d\alpha/dt)L/U$, where $d\alpha/dt$ represents a characteristic angular velocity (such as p, q or r). The Reynolds number describes the relative importance of viscous effects to inertial effects, the Froude number characterizes the ratio of hydrodynamic to hydrostatic restoring moments acting on the model, and the Strouhal number is a fundamental measure of the unsteadiness of the

motion. The subscripts s and m will denote the full scale ship and the model, respectively. We then wish to obtain:

$$\begin{aligned} (UL/\nu)_m &= (UL/\nu)_s && \text{Re scale} \\ \left(U/\sqrt{gL}\right)_m &= \left(U/\sqrt{gL}\right)_s && \text{Fr scale} \\ [(d\alpha/dt)\,L/U]_m &= [(d\alpha/dt)\,L/U]_s && \text{St scale} \end{aligned} \quad . \tag{1}$$

These equations show that since U and L appear both in the numerators and in the denominators of these quantities, they cannot be matched simultaneously. We have developed a new approach to address this technical challenge.

Basic Concepts

Ship motion is a response to forces and moments acting on a craft. A typical submarine configuration showing rudders, sternplanes, sail and the general shape of the hull is depicted in Fig. 1. The classic approach of satisfying geometric and kinematic similarities in model tests is intended to produce similar forces and moments at model and full scale to generate the same ship motions. Generating proper forces and moments acting on the model is the first priority in conducting model tests.

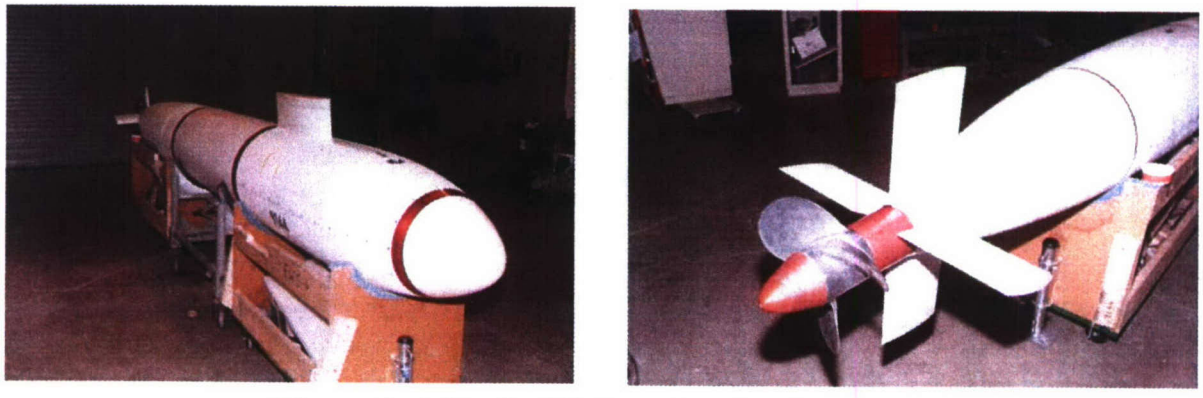

Figure 1. A Typical Submarine Configuration

The forces, moments and the corresponding ship motion can be expressed in terms of three linear and three angular differential equations similar in form to that which describes a spring-mass system. Furthermore, Lloyd (1989) has shown that for conventional surface ships in waves the product moments of inertia are usually small and negligible. Let F_i and M_i denote force and moment components, which will be normalized by $1/2\rho U^2 S$ and $1/2\rho U^2 S L$, respectively, where we use the symbols L and S to denote ship length and hull surface area. Let m_0 and I_0 denote ship mass and moment of inertia, and m_1 and I_1 denote virtual mass and moment of inertia. The quantities d^2x_i/dt^2 and $d^2\alpha_i/dt^2$ will denote linear and angular acceleration components. The index variables $i = 1,2,3$ and $i = 4,5,6$ will represent surge, sway and heave for linear motions and roll, pitch and yaw for angular motions, respectively. We then obtain:

$$\frac{F_i}{1/2\rho U^2 S} = \frac{(m_0 + m_1)\dfrac{d^2 x_i}{dt^2}}{1/2\rho U^2 S} \qquad i = 1,2,3 \quad \text{and}$$
$$\frac{M_i}{1/2\rho U^2 S L} = \frac{(I_0 + I_1)\dfrac{d^2 \alpha_i}{dt^2}}{1/2\rho U^2 S L} \qquad i = 4,5,6 \tag{2}$$

If normalized forces and moments on the left-hand-sides (LHS) of Eqs. 2 are the same for both the model and the ship, namely $LHS_m = LHS_s$, then

$$\left(\frac{F_i}{1/2\rho U^2 S}\right)_m = \left(\frac{F_i}{1/2\rho U^2 S}\right)_s \qquad i = 1,2,3 \quad \text{and}$$
$$\left(\frac{M_i}{1/2\rho U^2 S L}\right)_m = \left(\frac{M_i}{1/2\rho U^2 S L}\right)_s \qquad i = 4,5,6 \tag{3}$$

Equality of the forces and moments will then result in a vehicle response, *which must be the same* at model and full scale; namely, the inertia terms on the right-hand-sides (RHS) of Eqs. 2 will be the same and be given by

$$\left(\frac{(m_0 + m_1)\dfrac{d^2 x_i}{dt^2}}{1/2\rho U^2 S}\right)_m = \left(\frac{(m_0 + m_1)\dfrac{d^2 x_i}{dt^2}}{1/2\rho U^2 S}\right)_s \qquad i = 1,2,3 \quad \text{and}$$
$$\left(\frac{(I_0 + I_1)\dfrac{d^2 \alpha_i}{dt^2}}{1/2\rho U^2 S L}\right)_m = \left(\frac{(I_0 + I_1)\dfrac{d^2 \alpha_i}{dt^2}}{1/2\rho U^2 S L}\right)_s \qquad i = 4,5,6 \tag{4}$$

From Eqs. 4, scaling formulas or transfer functions can be derived to relate model data to full scale ship motion. The challenge will be to develop an experimental procedure for submarine model testing that can produce the same normalized forces and moments acting at both scales as specified in Eqs. 3.

Mathematical Formulation

First consider the angular motions. The linear motions will be treated later. Let α denote an Euler angle component, where $\alpha_i = (\varphi, \theta, \psi)$ and φ, θ and ψ represent roll, pitch, and yaw angles, respectively. The ship motion can be generalized in the form of a differential equation for a spring-mass system for each angle component as follows (refer to Fig. 1).

$$M_e + M_1(\alpha) + M_2\left(\frac{d\alpha}{dt}\right) = M_3\left(\frac{d^2\alpha}{dt^2}\right) = (I_0 + I_1)\frac{d^2\alpha}{dt^2}. \tag{5}$$

The term M_e refers to excitation moments from movable appendages such as rudders, sternplanes and a propulsor. The terms $M_1(\alpha)$, $M_2(d\alpha/dt)$ and $M_3(d^2\alpha/dt^2)$ denote the moments that are functions of flow angle, angular velocity, and angular acceleration, respectively. Equation 5 applies both at full scale and model scale, namely

$$\begin{aligned}\left[M_e + M_1(\alpha) + M_2\left(\frac{d\alpha}{dt}\right)\right]_s &= \left[(I_0 + I_1)\frac{d^2\alpha}{dt^2}\right]_s \\ \left[M_e + M_1(\alpha) + M_2\left(\frac{d\alpha}{dt}\right)\right]_m &= \left[(I_0 + I_1)\frac{d^2\alpha}{dt^2}\right]_m\end{aligned} \quad . \tag{6}$$

The first task in this study is to identify a test method such that forces and moments acting on the full scale vehicle are correctly represented at model scale, namely to achieve

$$\left[\frac{M_e + M_1(\alpha) + M_2\left(\frac{d\alpha}{dt}\right)}{\frac{1}{2}\rho U^2 SL}\right]_m = \left[\frac{M_e + M_1(\alpha) + M_2\left(\frac{d\alpha}{dt}\right)}{\frac{1}{2}\rho U^2 SL}\right]_s . \tag{7}$$

The next task will be to derive the scaling formulas to relate measured RCM data to full scale ship motions. This task is performed by equating the vehicle response on the right-hand-sides of Eqs. 6

$$\left[\frac{(I_0 + I_1)\frac{d^2\alpha}{dt^2}}{\frac{1}{2}\rho U^2 SL}\right]_m = \left[\frac{(I_0 + I_1)\frac{d^2\alpha}{dt^2}}{\frac{1}{2}\rho U^2 SL}\right]_s . \tag{8}$$

Test Procedure to Satisfy Dynamic Similarity Requirements

We will assume that forces and moments acting on a full scale vehicle can be simulated with RCM tests if Reynolds, Froude, and Strouhal numbers are preserved at each scale. Simulation of a ship in a planes-fixed turn will be used as an example to demonstrate the concepts and to develop a new RCM test procedure. A similar approach can be applied to rudder or sternplane jam recovery simulations. Note that a planes-fixed turn is one for which no automatic controller is used with the sternplanes to maintain a constant depth during the turn; instead, the sternplanes are maintained in a fixed position, and the depth is allowed to vary.

A sketch of craft trajectory and the corresponding response of the vehicle as described by time histories of ship speed, angular velocity, and accelerations in response to a rudder angle deflection are shown in Fig. 2 (Lewis, 1989). The terms v, β and r denote lateral velocity, drift angle and yaw angular velocity (turning rate). The terms $\dot{v}$ and $\dot{r}$ represent accelerations. The rudder is deflected with a constant deflection rate of $d\delta_r/dt$ to a specified angle δ_r as shown in

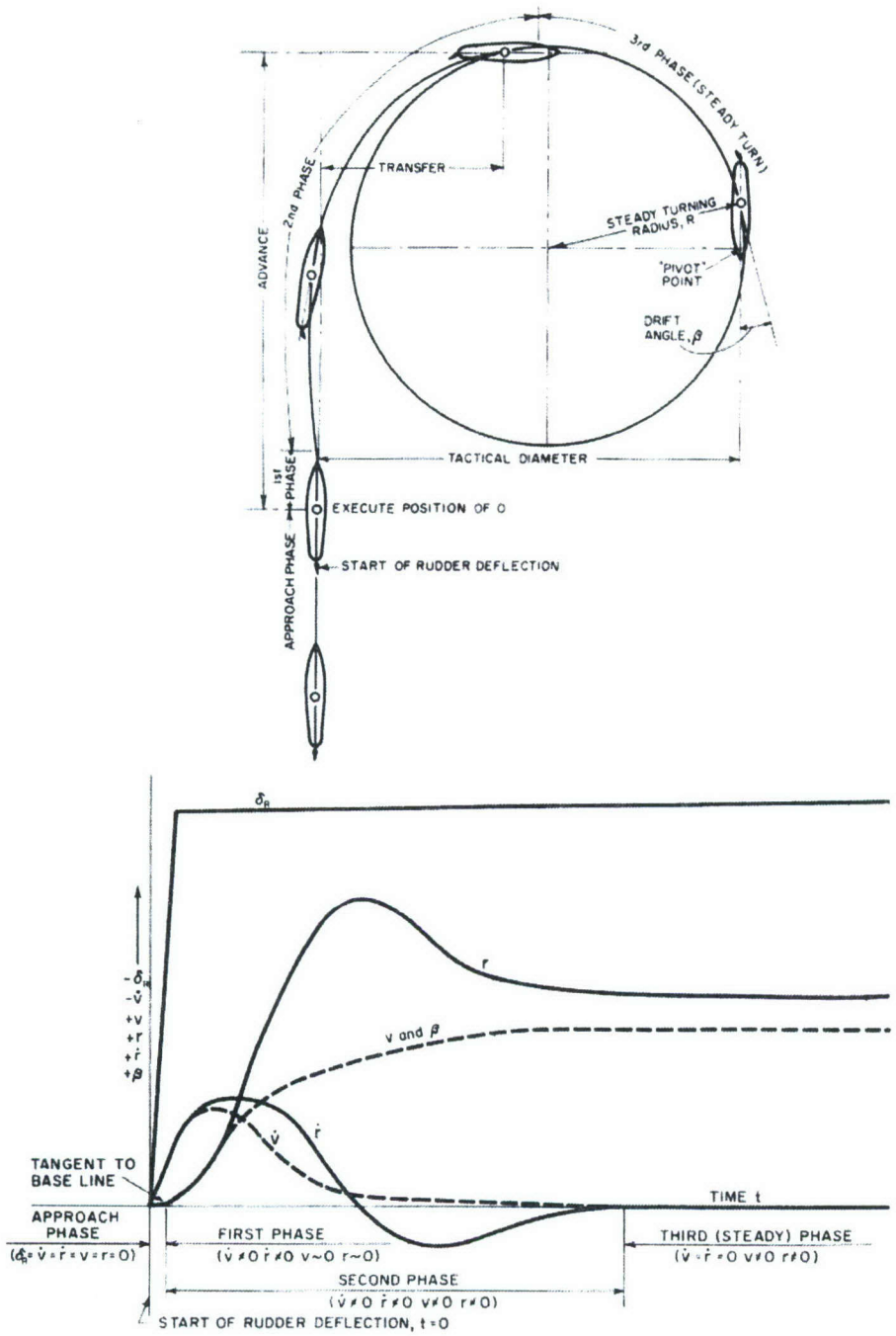

Figure 2. Turning Maneuver Description and Phases

Fig. 2. The craft motion is divided into three phases with the start of the rudder deflection representing the time origin, $t = 0$.

The first phase is dominated by the rudder deflection, and the ship response is primarily inertial. The second phase is associated with ship turning represented by the appearance of side velocity v and turning rate r. The quasi-steady turn, as demonstrated by the disappearance of inertial terms, signifies the third phase. To show a turning example, the symbols used in Eq. 6 are revised as

$$\left[\frac{M_e + M_1(v) + M_2(r)}{\frac{1}{2}\rho U^2 SL}\right]_m = \left[\frac{M_e + M_1(v) + M_2(r)}{\frac{1}{2}\rho U^2 SL}\right]_s, \tag{7a}$$

where v is the lateral velocity at the center of gravity (CG) and is obtained from $v = -U\sin\beta$.

Motivation for Reynolds Scale Simulation in RCM Tests

The requirement to match Reynolds numbers results from a consideration of Conservation of Momentum for the fluid in which the vehicle is moving. This physical law is expressed in the Navier-Stokes equations, and when these are made dimensionless, the Reynolds number arises as the key dimensionless group expressing the ratio of inertial to viscous forces. By matching this dimensionless group at both model and full scale, the governing equations for the fluid will then be identical and will result in similar solutions. As discussed above in Eq. 1, we must also match Froude and Strouhal numbers. As we proceed we will find that it is possible to match the latter two groups, but we cannot also match the Reynolds number simultaneously. Therefore, the two-order-of-magnitude difference in Reynolds number between model and full scale implies Reynolds scaling effects will appear at model scale for those motions where viscous effects are important. The impact of these effects will be to alter the force and moment distribution acting on the vehicle to various degrees. Although we cannot match Reynolds number, if we can assess how these force and moment changes are created by the appendages and the hull, then *we can correct them*. We will refer to this correction approach as *dynamically satisfying Reynolds number*. The next few subsections will evaluate the needed corrections on various appendages and the hull for a submarine turning maneuver.

Reynolds Scale Correction on Rudder Performance – First Phase

As noted in Fig. 2, the first phase of a turning maneuver is that short period of time when the vehicle motion is still governed by inertia and corresponds to $v \approx 0$, $r \approx 0$, $\dot{v} \neq 0$ and $\dot{r} \neq 0$. We can simplify Eq. 7a, to obtain

$$\left[\frac{M_e}{\frac{1}{2}\rho U^2 SL}\right]_m = \left[\frac{M_e}{\frac{1}{2}\rho U^2 SL}\right]_s. \tag{9}$$

Equation 9 requires that the dimensionless moments produced by rudders to turn the vehicles about their CG must be equal if the first phase of the turning maneuver is to be properly simulated in RCM tests.

As can be seen in Fig. 1, rudders are located at the aft end of the vehicle and are immersed in the boundary layer developed along the ship's hull. The ratio of the boundary layer thickness to the ship length is much greater for the model than for the full scale vehicle as shown by the typical profiles given in Fig. 3. The model rudder placed in the thicker boundary layer will develop a smaller force and moment than a full scale rudder. This Reynolds scale effect is associated with the boundary layer velocity deficit.

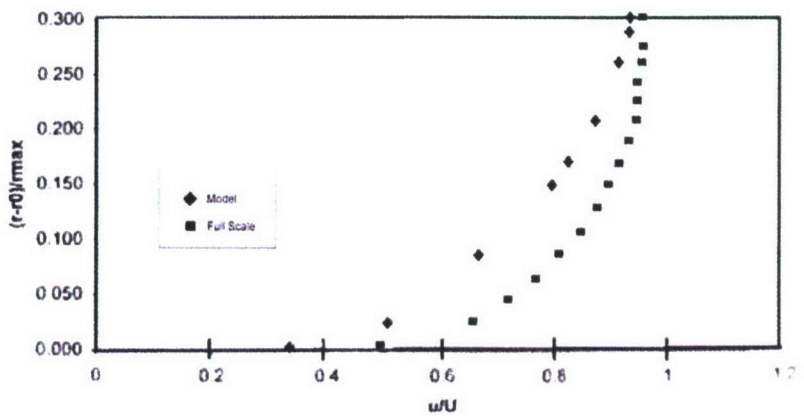

Figure 3. Boundary Layer Velocity Profiles at the Rudder Plane

Another scale effect acting on the rudder is related to the boundary layer displacement thickness. The Reynolds numbers based on mean rudder chord are around $Re = 0.5 \times 10^6$ for the model and $Re = 40 \times 10^6$ for a full scale rudder. Measurements on several NACA airfoils, shown in Fig. 4, exhibit significant scale effects on lift coefficients especially at low Reynolds numbers of less than 1×10^6 (Loftin and Smith, 1949; Loftin and Bursnall, 1950; and Whicker and Fehlner, 1958). The lift coefficients are seen to increase with Reynolds number. This trend is also observed theoretically by Spence (1954).

Consider a simple rectangular foil of chord length c and span s located in a non-uniform flow $u(y)$ as shown in Fig. 5. The section lift $\Delta £$ on a segment Δy due to an angle of attack δ_r is given by

$$\Delta £ = C_L \left[\frac{1}{2}\rho u^2(y)\right] c\,\Delta y = \frac{\partial C_L}{\partial \delta_r}\delta_r \left[\frac{1}{2}\rho u^2(y)\right] c\,\Delta y\,. \tag{10}$$

Taking the limit as $\Delta y \to 0$, we obtain

$$£ = \int \frac{\partial C_L}{\partial \delta_r}\delta_r \left[\frac{1}{2}\rho u^2(y)\right] c\,dy = \frac{1}{2}\rho c \delta_r \int \frac{\partial C_L}{\partial \delta_r}(y)\,u^2(y)\,dy\,, \tag{11}$$

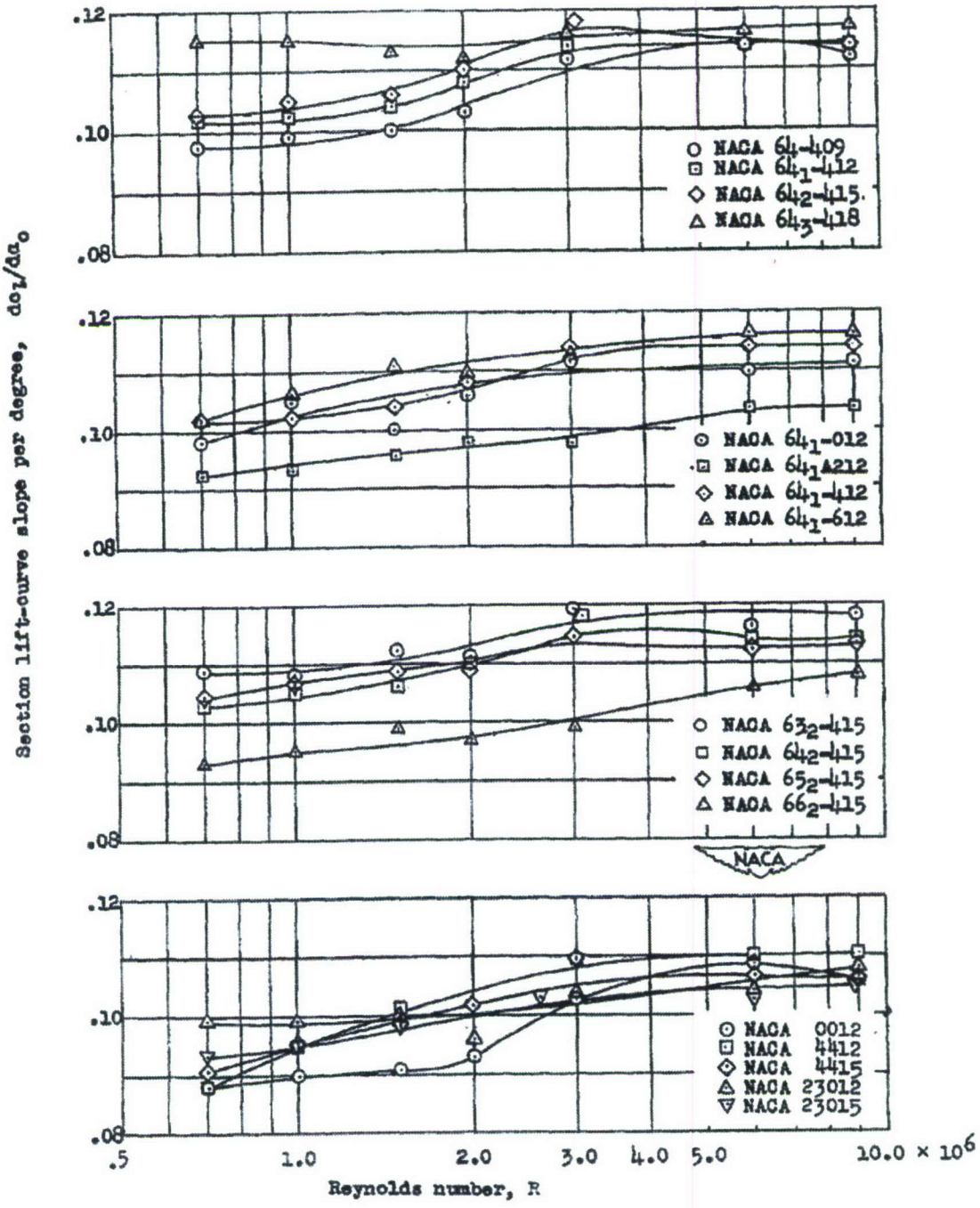

Figure 4. Variation of Lift Curve Slope of 17 Airfoils of Smooth Surfaces with Reynolds Numbers

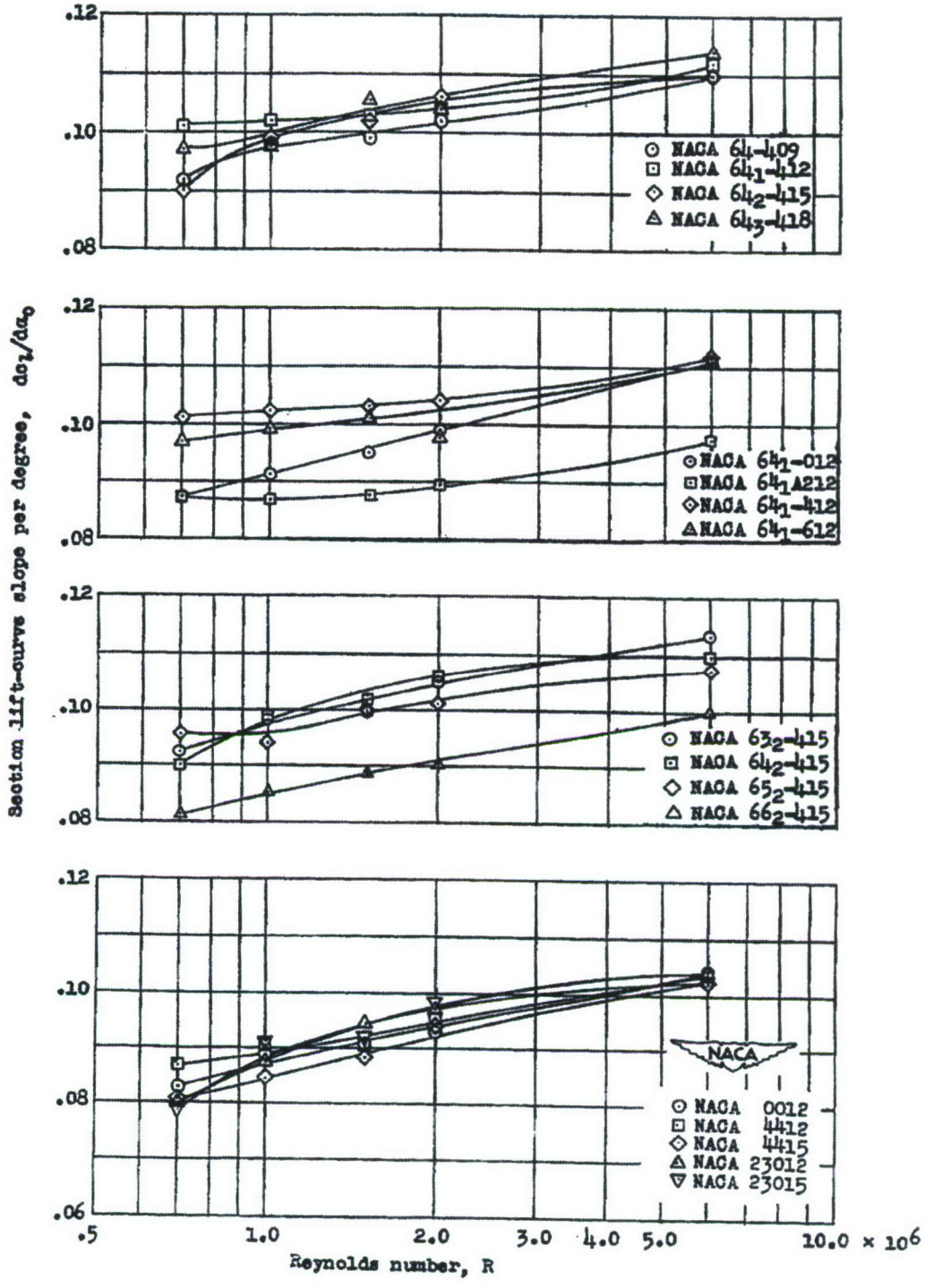

Figure 4 (Cont.). Variation of Lift Curve Slope of 17 Airfoils of Roughened Surfaces with Reynolds Numbers

where $\partial C_L/\partial \delta_r(y)$ denotes the lift curve slope, which varies along the span as a result of the boundary layer velocity gradient. However, the weak variation in $\partial C_L/\partial \delta_r(y)$ in the boundary layer at model scale is *much smaller* than the variation resulting from a two-order-of-magnitude Reynolds number difference between model and full scale. Hence, we will replace the weak boundary layer variation with a mean value, $\overline{\partial C_L/\partial \delta_r}$, and remove it from the integral.

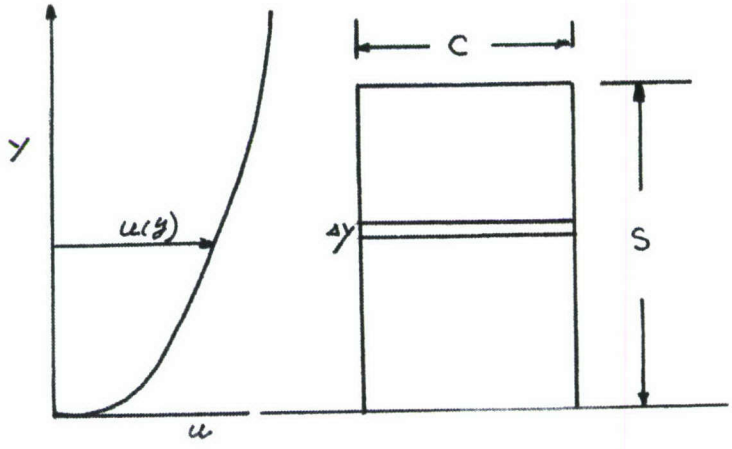

Figure 5. Boundary Layer Effect on Lifting Surfaces

We obtain

$$£ = \frac{1}{2}\rho c \delta_r \overline{\frac{\partial C_L}{\partial \delta_r}} \int_0^s u^2(y)\,dy\,. \tag{12}$$

Shift now to dimensionless variables $u' = u/U$ and $y' = y/s$ to get

$$£ = \frac{1}{2}\rho c \delta_r \overline{\frac{\partial C_L}{\partial \delta_r}} U^2 s \int_0^1 u'^2(y')\,dy'\,. \tag{13}$$

Let the rudder area be denoted by $A_r = cs$ and divide both sides by hull surface area S to get a normalized lift given by

$$\frac{£}{\frac{1}{2}\rho U^2 S} = \frac{A_r}{S}\delta_r \overline{\frac{\partial C_L}{\partial \delta_r}} \int_0^1 u'^2(y')\,dy'\,. \tag{14}$$

Use X_r to denote the distance between the rudder and the center of gravity of the vessel. Multiply both sides by X_r/L to get a normalized turning moment in the form

$$\left[\frac{M_e}{\frac{1}{2}\rho U^2 SL}\right]_s = \left[\frac{£X_r}{\frac{1}{2}\rho U^2 SL}\right]_s = \left[\frac{X_r}{L}\frac{A_r}{S}\delta_r\frac{\overline{\partial C_L}}{\partial\delta_r}\int_0^1 u'^2(y')dy'\right]_s \quad \text{ship}$$

$$\left[\frac{M_e}{\frac{1}{2}\rho U^2 SL}\right]_m = \left[\frac{£X_r}{\frac{1}{2}\rho U^2 SL}\right]_m = \left[\frac{X_r}{L}\frac{A_r}{S}\delta_r\frac{\overline{\partial C_L}}{\partial\delta_r}\int_0^1 u'^2(y')dy'\right]_m \quad \text{model} \qquad (15)$$

where the subscripts are used to represent the equations evaluated at full and model scales. By now substituting the above equations into Eq. 9 and noting that $[X_r/L]_s = [X_r/L]_m$ we obtain

$$[\delta_r]_m = [\delta_r]_s \frac{\left[\frac{A_r}{S}\right]_s}{\left[\frac{A_r}{S}\right]_m}\frac{\left[\frac{\overline{\partial C_L}}{\partial\delta_r}\right]_s}{\left[\frac{\overline{\partial C_L}}{\partial\delta_r}\right]_m}\frac{\left[\int_0^1 u'^2(y')dy'\right]_s}{\left[\int_0^1 u'^2(y')dy'\right]_m}$$

$$[\delta_r]_m \equiv [\delta_r]_s \frac{\left[\frac{A_r}{S}\right]_s}{\left[\frac{A_r}{S}\right]_m}\xi\,\eta \qquad (16)$$

where ξ denotes the Reynolds scale effect on rudder lift as a result of boundary layer displacement thickness, and η the scale effect due to the difference in the hull boundary layers at each scale. Summarizing, we have

$$\xi \equiv \frac{\left[\frac{\overline{\partial C_L}}{\partial\delta_r}\right]_s}{\left[\frac{\overline{\partial C_L}}{\partial\delta_r}\right]_m} \quad \text{and} \quad \eta \equiv \frac{\left[\int_0^1 u'^2(y')dy'\right]_s}{\left[\int_0^1 u'^2(y')dy'\right]_m}, \qquad (17)$$

A Reynolds-averaged Navier-Stokes (RANS) code was used to calculate boundary layer velocity profiles on three vessels. The numerical results for η are shown in Table 1 and are found to be sensitive to hull shape with values ranging from 1.06 to 1.16.

Table 1. Values for $\eta = \left[\int_0^1 u'^2(y')dy'\right]_s \Big/ \left[\int_0^1 u'^2(y')dy'\right]_m$

	Top Rudder	Bottom Rudder
Ship I	1.06	1.09
Ship II	1.12	1.16
Ship III	1.07	1.08

The effect of Reynolds scale on lift curve slope ξ has been calculated theoretically by Spence on a two dimensional Joukowski airfoil at a $6°$ attack angle and is shown in Fig. 6. The value of ξ is estimated to be around $\xi \approx 1.13$ for a model Reynolds number of $Re = 0.5\times10^6$ and a full scale value of $Re = 40\times10^6$. Thus, a significant viscous effect on rudder force is noted. Two methods to satisfy Eq. 16 are presented.

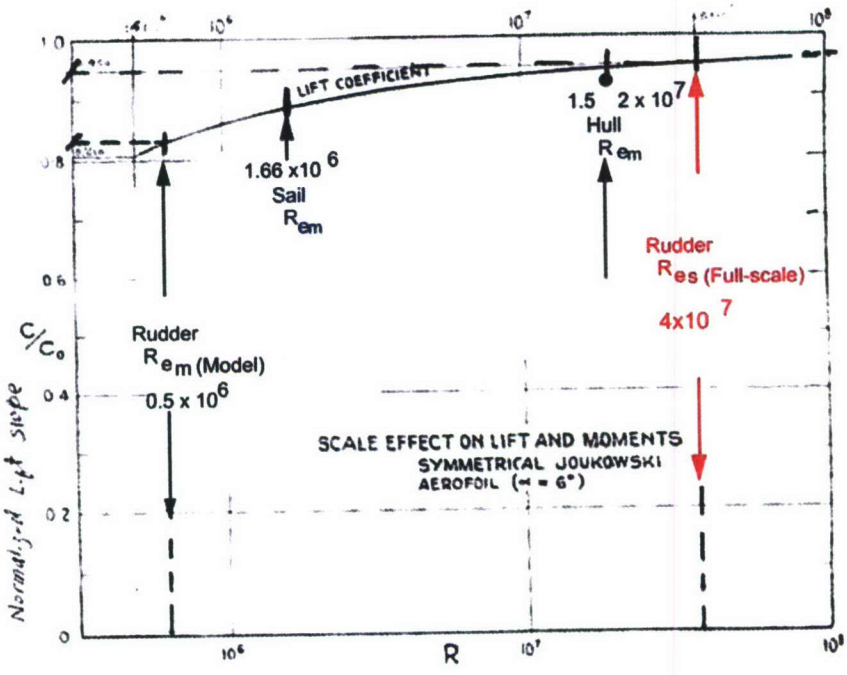

Figure 6. Reynolds Number Effect on Lift Slope

Method 1

Modify the rudder deflection angle in the RCM test. For this case, the model rudder is constructed to be geometrically similar to that for full scale, namely $[A_r/S]_s = [A_r/S]_m$, and Eq. 16 becomes

$$[\delta_r]_m = [\delta_r]_s\, \xi\, \eta, \quad \text{where } \xi > 1 \text{ and } \eta > 1. \tag{18}$$

As a numerical example, consider the case of a full scale vessel conducting a turning maneuver with a rudder deflection of $[\delta_r]_s = 25°$. To compensate for the Reynolds scale effect on rudder force and turning moment, the model rudder must be deflected to

$$\begin{aligned} [\delta_r]_m &= [\delta_r]_s\, \xi\, \eta = (25)(1.13)(1.06) = 30° \quad \text{for one hull shape, and} \\ [\delta_r]_m &= [\delta_r]_s\, \xi\, \eta = (25)(1.13)(1.16) = 33° \quad \text{for another hull shape} \end{aligned} \tag{19}$$

Note carefully that the values of ξ and η used in this example are just for demonstration. More accurate values will need to be obtained from a correlation study of full scale and RCM maneuvering data.

Method 2

Modify the rudder size for the RCM model. In this approach, the rudder deflection angles for execution of the turn will be the same for RCM tests and for full scale trials. That is, we will set $[\delta_r]_m = [\delta_r]_s$, and Eq. 16 becomes

$$\begin{aligned} &\frac{\left[\frac{A_r}{S}\right]_s}{\left[\frac{A_r}{S}\right]_m} \xi\, \eta = 1 \text{ , or} \\ &\frac{[A_r]_m}{[A_r]_s} = \frac{[S]_m}{[S]_s} \xi\, \eta = (1/\lambda^2)\xi\, \eta = \begin{cases} 1.20/\lambda^2 & \text{one hull shape} \\ 1.31/\lambda^2 & \text{another hull shape} \end{cases} \end{aligned} \tag{20}$$

where $\lambda = L_s/L_m$ is the length scale ratio between full and model scales. This implies that the scale effect on rudder force and moment can be mitigated if the rudder on the RCM model is made 20-31% greater in area than a geometrically similar rudder.

Second Phase of a Turning Maneuver

The second phase of a turning maneuver corresponds to conditions where the vehicle begins to respond to the rudder deflection with lateral and yawing motions such that $v \neq 0, r \neq 0, dv/dt \neq 0$ and $dr/dt \neq 0$. Under these conditions, we return to Eq. 7a to establish the dynamic scaling requirement:

$$\left[\frac{M_e + M_1(v) + M_2(r)}{\frac{1}{2}\rho U^2 SL}\right]_m = \left[\frac{M_e + M_1(v) + M_2(r)}{\frac{1}{2}\rho U^2 SL}\right]_s . \tag{7a}$$

The presence of nonzero v and r terms will produce varying flow attack angles along the ship hull, sail and control appendages, such as rudders and sternplanes.

Reynolds Scale Correction on Sail Performance

At model scale, the sail typically operates at a Reynolds number of $\mathrm{Re}_m = 1.5 \times 10^6$. Let u, v, and w denote velocity components at the ship center of gravity (CG). The angular velocities for roll, pitch, and yaw motions will be given by p, q, and r. Let X_{sail} be the distance between the CG of the ship and the sail, such that it represents the moment arm for turning. Z_{sail}, a positive-definite scalar, will denote the vertical distance between the location of the resultant force produced by the sail and the x-axis of the ship, thereby denoting a moment arm for roll. The side slip angle β at the sail can be calculated by

$$v_{sail} = v + pZ_{sail} + rX_{sail}$$
$$\beta = \sin^{-1}\left(\frac{-v_{sail}}{U}\right) \quad . \tag{21}$$

Dynamic lift will be produced by the sail due to the angle of attack, β. A sail is typically located forward of the CG of the ship where the boundary layer that develops along the ship's hull is still relatively thin. Using a typical 1/7th power law turbulent boundary layer velocity profile, a value of $\eta \approx 1.02$ may be estimated on the ONR Body 1 sail using available geometrical information, (Faller and Merrill, 2001). A value of $\xi \approx 1.07$ is estimated by applying Spence's data provided in Fig. 6 for $\mathrm{Re}_m = 1.5 \times 10^6$. Using these two values for ξ and η and the method described in Eq. 20, we can correct the Reynolds scale effect on the sail

$$\frac{[A_r]_m}{[A_r]_s} = \frac{[S]_m}{[S]_s} \xi \eta = 1.09/\lambda^2 \, . \tag{22}$$

Equation 22 indicates that the scale effect on the force and moment produced by the sail on the RCM model can be mitigated by making the model sail 9 % greater than a geometrically similar sail.

Reynolds Scale Correction on Ship Hull Performance

At model scale, the ship's hull typically operates at a Reynolds number of $\mathrm{Re}_m = 1.5 \times 10^7$. Steady flows over axisymmetric bodies at an angle of attack have received considerable attention both theoretically and experimentally in the areas of three dimensional flow separation, the formation of leeward vortices and the unsteadiness around separation zones (Bridges, 2003; Fu et al, 1994; Han and Patel, 1979). A 6:1 prolate spheroid undergoing time dependent maneuvers was tested by Hoang, et al. (1994) using their Dynamic Plunge-Pitch-Roll (DyPPiR) facility at a Reynolds number of $\mathrm{Re}_m = 4.2 \times 10^6$. Their data showed that unsteady flow separation phenomena were significantly different from those associated with steady separation. Furthermore, airfoils at an angle of attack in unsteady flow exhibit significantly delayed flow separation (Shen and Fuhs, 1999). Lloyd (1989) observed on surface ships that viscous forces play a less important role in ship motion dynamics. Two turning cases are

considered. One corresponds to a gentle turn with small v and r terms, and the other corresponds to a tight turn with large v and r terms.

Gentle Turn

There is no scale effect on the ship's hull due to the boundary layer velocity deficit term, namely $\eta = 1$. It is further noted from unsteady experimental data that the flow angles associated with flow separation observed in steady tests are greatly delayed. For a gentle turn, drift angle at all locations along the hull is small, and cross flow may not play a significant role in producing force and moment. Based on the theories of Spence (1954), Howarth (1935) and Bridges, et al. (2003), $\xi \approx 1.01$ to 1.02 is estimated for the ship hull at $\mathrm{Re}_m = 1.5 \times 10^7$. Using these two values for ξ and η and the method described in Eq. 20, the Reynolds scale effect on the hull may be estimated to be

$$\lambda^2 \frac{[A_{hull}]_m}{[A_{hull}]_s} = \xi\,\eta = 1.01 \text{ to } 1.02 . \tag{23}$$

The scale effect on ship hull is small. This is in agreement with general observations in straight line and rotating arm data. If model experiments are performed at Reynolds numbers greater than 10 to 15 million, then scale effects between model and full scale appear to be negligible for the purpose of making stability and control predictions.

Tight Turn

During a tight turn, accompanied by larger v and r terms, large flow angles as much as 20 to 30 degrees may be encountered at the ship stern. Therefore, cross flow separation may be an issue. The degree to which scale effects play a role in the cross flow separation for RCM maneuvering tests at $\mathrm{Re}_m = 1.5 \times 10^7$ is not clear. This is an area which warrants further study. Surface roughness (grit) has been applied to the RCM hull and has demonstrated considerable influence on turning maneuvers. If scale effects on cross flow separation should prove to be large in RCM experiments, then a closer examination of distributed hull roughness should be carried out. Another possibility is the application of a thin wire along the side of the ship hull to trigger a supercritical flow pattern as demonstrated in a sphere experiment (Schlichting, 1979). The resulting transition to turbulent cross flow can greatly modify cross flow drag.

Reynolds Scale Correction on Rudder Performance – Second Phase

Equation 7a describes the moments to be matched between model and full scales. The simpler Eq. 9 was obtained by removing terms that are negligible. The remaining term, the exciting moment, results from the rudder deflection. During the second phase of the turn, nonzero lateral and yawing motions modify the moment produced by the rudder deflection such that it may be said to originate from a smaller *effective* rudder angle. Further, this effective rudder angle changes continuously in time (grows smaller) while the ship is in a turn as v and r grow in magnitude. Let δ_r denote the geometric rudder angle with respect to the ship centerline.

The effective rudder angle $\delta_{r\,eff}$ is defined by the difference of the geometric rudder angle and a correction term which represents the instantaneous flow angle acting on the rudder

$$\begin{aligned}\delta_{r\,eff} &= \delta_r - c(v,r) \\ &= \delta_r - \tan^{-1}\left[\frac{-v - rX_r}{u}\right],\end{aligned} \tag{24}$$

where X_r, a positive-definite scalar, is the distance from the CG aft to the rudder. Following Eq. 18 for geometrically similar rudders, we now use the effective rudder angle to get

$$\begin{aligned}\left[\delta_{r\,eff}\right]_m &= \left[\delta_{r\,eff}\right]_s \xi\,\eta \\ \left[\delta_r - c\right]_m &= \left[\delta_r - c\right]_s \xi\,\eta \\ \left[\delta_r\right]_m - \left[c\right]_m &= \left(\left[\delta_r\right]_s - \left[c\right]_s\right)\xi\,\eta \quad \text{but } \left[c\right]_m = \left[c\right]_s = c\,. \\ \left[\delta_r\right]_m &= \left[\delta_r\right]_s \xi\,\eta - c(\xi\,\eta - 1) \\ \left[\delta_r\right]_m &= \left[\delta_r\right]_s \xi\,\eta - \tan^{-1}\left[\frac{-v - rX_r}{u}\right](\xi\,\eta - 1)\end{aligned} \tag{25}$$

The last of Eqs. 25 gives the angle to which the rudder should be set at model scale to produce the same exciting moment as that obtained at full scale. The correction for scale effects given by Eq. 18 for phase 1 and by Eq. 25 for phase 2 should be applied at each instant of time. However, during phase 2, as v and r grow in magnitude, the effective rudder angle decreases as does the exciting moment implying that the need for scale effect correction diminishes. Thus, we propose a rudder angle correction as shown in Fig. 7, which is larger during Phase 1 and the early part of Phase 2, but decreases in magnitude as the turn proceeds. The details of the shape of the correction can be refined after conducting model tests.

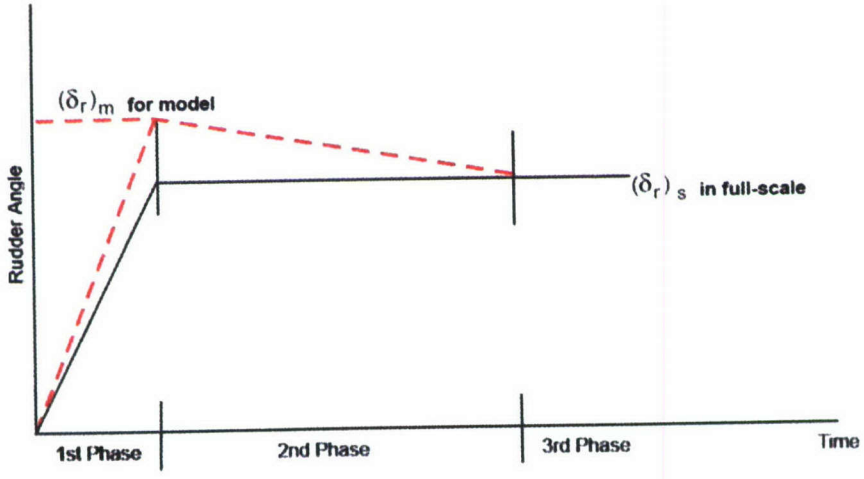

Figure 7. Proposed Rudder Deflection in Model Tests for Reynolds Scale Correction

Table 2 summarizes the estimated magnitudes of Reynolds scale effect corrections on the exciting moments produced by rudders, sternplanes, the sail, and the ship hull.

Table 2. Reynolds Scale Effects

Item	ξ	η	$\xi\eta$
Rudder	1.13	1.06 ~1.16	1.20 ~1.31
Sternplane	1.13	1.06 ~1.16	1.20 ~1.31
Sail	1.07	1.02	1.09
Hull	1.01~1.02	1.00	1.01~1.02

Motivation for Froude Scale Simulation in RCM Tests

For submarines, the size of the top rudder is typically greater than the bottom rudder. Both rudders are linked such that they respond with the same rudder angle when executing a turn. When a turn is initiated, a roll moment is produced from the different size rudders, and the ship will experience roll motion in addition to yawing. A hydrostatic restoring moment is then induced resulting from the couple produced by weight acting at the CG and buoyancy acting at the center of buoyancy (CB). Buoyancy is expressed by $B = \rho V g$, where V is the volume of the ship. For a submarine, the CB is located a distance Z_{BG} directly above the CG, and this metacentric height (reduced by the sine of the roll angle) serves as the moment arm for the restoring moment. Let φ denote the ship roll angle. The similarity requirement to ensure the same dimensionless restoring moments during the turn can be expressed by

$$\left[\frac{\rho V g Z_{BG}\sin\varphi}{1/2\rho U^2 S L}\right]_m = \left[\frac{\rho V g Z_{BG}\sin\varphi}{1/2\rho U^2 S L}\right]_s . \tag{26}$$

Eq. 26 will be satisfied if

$$\left[\frac{g Z_{BG}}{U^2}\right]_m = \left[\frac{g Z_{BG}}{U^2}\right]_s \text{ and } [\varphi]_m = [\varphi]_s . \tag{27}$$

The first condition of Eq. 27 states that the model must be tested at *Froude scale*. A test method to ensure that Froude scale is preserved during RCM testing will be discussed later. The second condition of Eq. 27 requires that the angle experienced during roll motion at model scale must be the same as that measured at full scale. The conditions needed to satisfy these requirements during RCM testing will be examined.

Motivation for Strouhal Scale Simulation in RCM Tests

A ship in a turn develops angular velocities in roll, pitch and yaw associated with the $M_2(r)$ term. Unsteady lift and moment are produced as a result. The dynamic lift on an airfoil in a sinusoidal pitching motion has been theoretically investigated in an inviscid fluid by

Theodorsen (1935). His theory shows that the dynamic lift and the phase angle with respect to the instantaneous foil angle is uniquely defined by the reduced frequency K defined by

$$K = \frac{\omega C}{2U}, \tag{28}$$

where ω, C, and U denote the oscillation frequency of the attack angle variation, chord length, and free stream speed, respectively.

During RCM maneuvering tests, the motion in the second phase of the turning maneuver is unsteady. The angular velocity $d\alpha/dt$ is not constant, but is changing continuously with time. Experience shows that the unsteady forces and moments can be characterized by a Strouhal number St as follows (Schlichting, 1979 and Blake, 1984),

$$St = \frac{d\alpha}{dt}\frac{L}{U}, \tag{29}$$

Matching the Strouhal scale requires that

$$\left[\frac{d\alpha}{dt}\frac{L}{U}\right]_m = \left[\frac{d\alpha}{dt}\frac{L}{U}\right]_s. \tag{30}$$

Equation 30 is an important equation to be satisfied in model tests, if the amplitude and phase of the unsteady forces and moments are to be correctly simulated at model scale. To satisfy Eq. 30, we will make a prudent choice that

$$\left[\frac{d\alpha}{dt}\right]_m = \left[\frac{d\alpha}{dt}\right]_s \frac{U_s}{U_m}. \tag{31}$$

Substituting the right-hand side of Eq. 31 into the left-hand side of Eq. 30 will then dictate that:

$$\left[\frac{L}{U^2}\right]_m = \left[\frac{L}{U^2}\right]_s. \tag{32}$$

Therefore, the angular velocity to be experienced by the RCM model must be maintained at an angular velocity experienced by the ship multiplied by a factor of U_s/U_m. We will see in a later section that Eq. 32 can be satisfied by matching the Froude number and that Eq. 31 will then follow as a result of this matching.

These are the requirements that ensure that unsteady motions are correctly simulated in RCM tests. Methods to satisfy these two requirements will be discussed in a later section.

Crashback in Sternplane (Rudder) Jam Recovery Simulation

During the process of recovery from a sternplane jam, a large rudder deflection is typically executed to turn the ship sideways to produce a large drift angle and large form drag to

slow the ship. This is often followed by a rapid reversal of direction of propeller rotation (RPM reversal) to produce a large negative thrust to decelerate and stop the ship. This type of maneuver where the propeller is in reverse but the vehicle still has forward velocity is termed crashback. Thus, a major distinction between a conventional turning maneuver and a crashback maneuver is the propeller RPM reversal. As an example we will use a model test, which is conducted for the purpose of correlating with known full scale crashback maneuvers conducted during trials of the full scale vessel. Therefore, we assume that time histories of full scale ship speed, RPM, velocity components, attitude and trajectory are known. Generally, after extensive earlier predictions prior to full scale trials are provided to the fleet, a series of model scale casualty recovery maneuvers are carried out after full scale trials to validate the reliability of the RCM simulation capability. The procedure discussed here makes use of the latter as an example, but the method can be reversed so that RCM tests can be used for full scale predictions prior to trials.

Notional time histories of full scale ship speed $U_s(t_s)$ and propeller RPM $N_s(t_s)$ as a function of full scale time t_s are sketched in Fig. 8. Prior to execution of a sternplane jam recovery, the steady ship speed and RPM during the approach are denoted by U_{s0} and N_{s0}. Let t_{s0} denote the time when the RPM reversal is executed, and t_{s1} the time when the propeller speed drops to zero. At time t_{s2}, the propeller reaches a new prescribed speed of $N_{s\,rev}$ (the subscript *rev* refers to the reversed negative RPM) and is then maintained at this constant negative value. As a result, the ship experiences a sharp drop in ship speed as noted in Fig. 8.

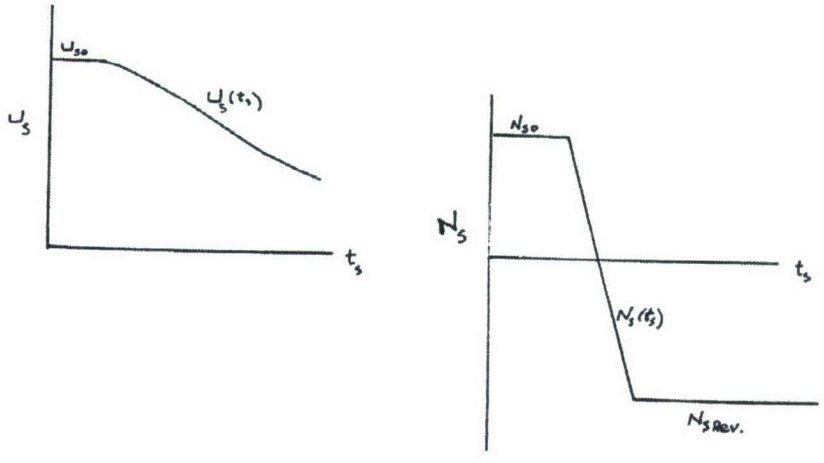

Figure 8. Full Scale Ship Speed and Propeller RPM Reversal Given $U_s(t_s)$ and $N_s(t_s)$

Existing RCM Test Procedure for Jam Recovery Simulation

As in a full scale jam recovery, a steady approach speed is required for RCM correlation maneuvers. The scaled model approach speed must be set at

$$U_{m0} = \frac{U_{s0}}{\sqrt{\lambda}}, \tag{33}$$

where $\lambda = L_s / L_m$ is the length scale ratio between full and model scales, and we will defer the explanation of Eq. 33 until a later section in Eq. 43.

Now, let J denote a propeller advance coefficient defined as $J = U/ND_p$, where D_p represents the propeller diameter. In an ideal fluid, the propeller RPM required to match advance coefficients at each scale,

$$\left[\frac{U}{ND_p}\right]_m = \left[\frac{U}{ND_p}\right]_s, \tag{34}$$

is then expected to produce the same thrust coefficient at each scale. However, in a real fluid, as a result of viscous effects, the ship hull drag coefficient C_r is greater at model scale than it is at full scale, $\left([C_r]_m > [C_r]_s\right)$. So, the propeller must produce additional thrust to overcome the additional drag at model scale. In other words, the propeller requires additional RPM in a real fluid than for the ideal fluid case, and therefore must operate at a lower propeller advance coefficient, $J_m < J_s$.

The required RPM at model scale is given by

$$N_{m0} = K_0 N_{s0} \sqrt{\lambda}, \tag{35}$$

where K_0 is a coefficient such that $K_0 > 1$. The value of K_0 depends on the hull form geometry and ship speed. Typically, K_0 is obtained from model tests.

At time t_{m0} the propeller reversal is executed. (Note that the relationship between model scale time t_m and full scale time t_s will be provided in a later section.) At time t_{m2} and thereafter, propeller rotation speeds in the existing procedure are set by using

$$N_{m\,rev} = N_{s\,rev} \sqrt{\lambda}, \tag{36}$$

Shown in Fig. 9 is a time history of model speed resulting from the above procedure that has been (Froude) scaled to the full scale range and then compared with the target full scale time history to be matched. As noted in the sketch, the time history of predicted ship speed can differ from the target ship speed by as much as 12% to 14%. Since dynamic forces are proportional to speed squared, significant error in the simulation of hydrodynamic forces and moments can be present in RCM correlation tests. This problem results from the fact that, while the approach speed is properly Froude scaled, the necessary Froude-scaled speed at each instant of time throughout the maneuver is not preserved during RCM tests. A method to preserve the Froude-scaled speed during RCM testing is presented next.

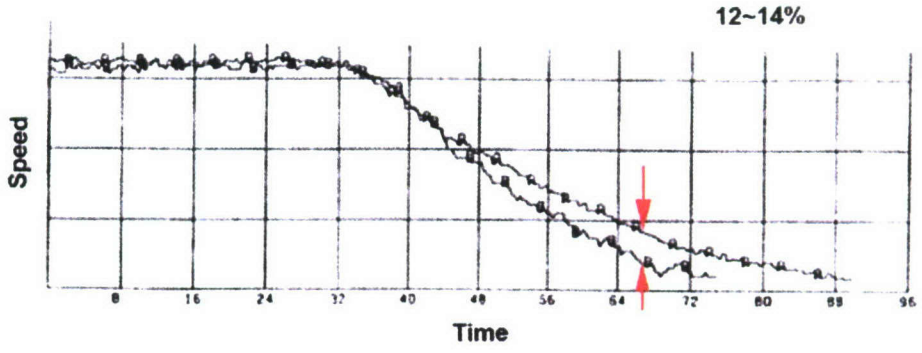

Figure 9. Model Measured vs. Target Ship Speed

Proposed RCM Test Procedure for Jam Recovery Simulation

The procedure to establish the approach speed is the same for the new method as it is in the existing approach. However, the reversal procedure is different. Consider the motion along the body x-axis. Let T and t denote propeller thrust and thrust deduction. A negative sign is assigned to the reversed thrust to indicate that it now acts in the same direction as the body resistance since the vehicle is still moving forward. Since, the thrust deduction is not sensitive to viscous effects, we find that

$$\left[\frac{-T(1-t)-R}{1/2\rho U^2 S}\right]_m = \left[\frac{-T(1-t)-R}{1/2\rho U^2 S}\right]_s . \tag{37}$$

Expressed in dimensionless form, we obtain

$$[C_T]_m = [C_T]_s - \frac{[C_R]_m - [C_R]_s}{1-t} . \tag{38}$$

During the early stage of the RPM reversal while the vehicle still maintains an appreciable forward speed, $[C_R]_m > [C_R]_s$ and $1-t>0$, which then dictates that

$$[C_T]_m > [C_T]_s . \tag{39}$$

So, we find that the reverse thrust produced by the model is too large, and as a result of scale effects acting to increase model resistance, less negative thrust is required during the early stage of the RPM reversal. Instead, we propose to modify Eq. 36 with

$$N_{m\,rev} = K(t_s)\, N_{s\,rev}\sqrt{\lambda} , \tag{40}$$

where $K(t_s)$ is a time varying coefficient.

The RCM model is operated under digital closed-loop control with two-way communications from the vehicle to an operations center accomplished by using radio signals. Therefore, the ship speed and RPM data can be up linked in real time. This means that RPM can be adjusted during a maneuver to ensure that the Froude-scaled model speed agrees with the target speed. The behavior of $K(t_s)$ is likely to depend on hull form and Reynolds numbers, and validation with experiments will be required to determine the shape of the $K(t_s)$ function.

During the later stage of the RPM reversal, ship speed has decreased from the level maintained during the approach. Furthermore, the negative reversed thrust produced by the propeller will now be substantially greater than the ship resistance. Hence, the needed thrust coefficient is likely to now be the same at model and full scale. We expect, therefore, that $K(t_s) \rightarrow 1$ towards the end of the maneuver. A sketch of the modified shape of the RPM function is provided in Fig. 10.

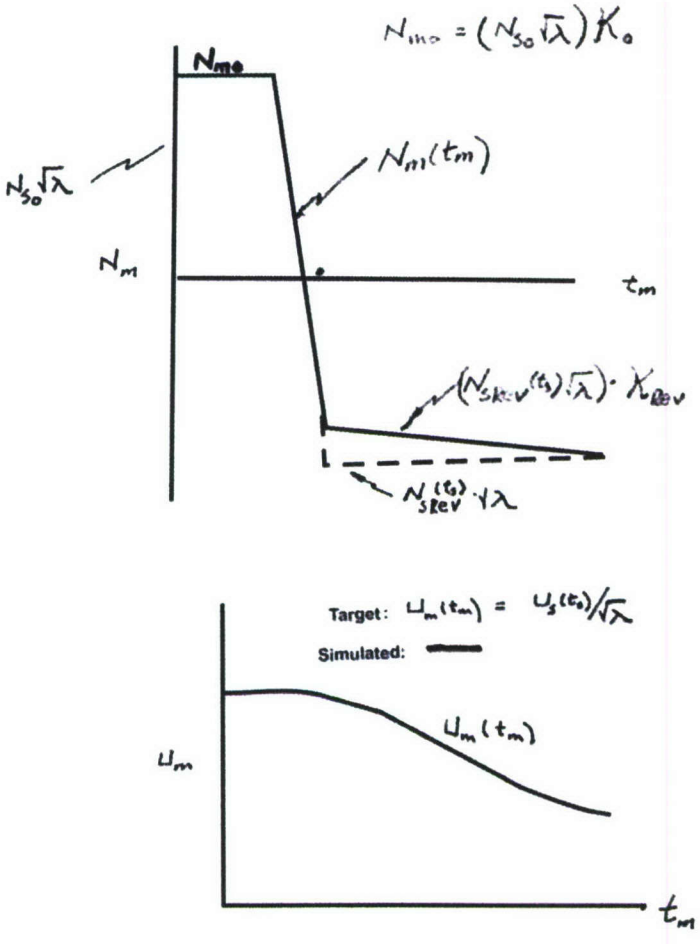

Figure 10. Proposed Procedure to Set Model RPM

Summarizing, the existing approach for establishing the RPM level in crashback simulation is based on using the same propeller advance coefficients for model and full scale propellers, namely $J_m = J_s$. In the proposed approach, the RPM will be adjusted such that Froude-scaled speed is preserved during the maneuver. We will see in the next section that this also has the benefit of preserving the Strouhal scale as well.

Transfer Functions (Scaling Formula)

The fundamental purpose of model testing is to use the model data to predict full scale performance. The formulas to relate model and full scale ship performance are termed transfer functions or scaling formulas. These are now derived.

The dynamic equations for linear and angular motions are given in Eqs. 2. We postulate that if the LHS of equations representing the forces and moments acting on the ship are simulated in model tests, namely if $LHS_m = LHS_s$, then the motions experienced by the ship will be duplicated by the model $RHS_m = RHS_s$. The relationship between full scale and model scale behavior can be deduced from these response functions. The derivation of the transfer functions will start with linear motion.

Linear Acceleration Scaling

Consider the x-component of linear motion given in Eqs. 4

$$\left(\frac{(m_0 + m_1)\frac{d^2x}{dt^2}}{1/2\rho U^2 S} \right)_m = \left(\frac{(m_0 + m_1)\frac{d^2x}{dt^2}}{1/2\rho U^2 S} \right)_s . \tag{4}$$

Let $a = d^2x/dt^2$ denote the linear acceleration. Although added mass is associated with the transformation of kinetic energy in ship motion, viscous effects associated with this quantity are small [Szebehely, 1952, 1953]. Equation 4 may be simplified to

$$\frac{a_s}{a_m} = \frac{[m_0 + m_1]_m}{[m_0 + m_1]_s} \frac{[\rho U^2 S]_s}{[\rho U^2 S]_m} \approx \frac{[m_0]_m}{[m_0]_s} \frac{[\rho U^2 S]_s}{[\rho U^2 S]_m} = \frac{U_s^2}{U_m^2} \frac{L_m}{L_s} . \tag{41}$$

A comparison of Eqs. 41 and 27 suggests that the solution for linear acceleration can be set by

$$\frac{a_s(t_s)}{a_m(t_m)} = 1 \quad \text{and} \quad U_s^2 = U_m^2 \frac{L_s}{L_m} . \tag{42}$$

We see that the time history of linear acceleration measured at model scale is directly applicable to full scale with the proper time scale applied.

Linear Velocity Scaling

To satisfy Eqs. 27, 32 and 42 requires that the model be tested at a speed given by

$$U_m(t_m) = \frac{U_s(t_s)}{\sqrt{\lambda}} \quad \text{or} \quad U_s(t_s) = \sqrt{\lambda}\, U_m(t_m), \tag{43}$$

where $\lambda = L_s / L_m$ is the length scale ratio between full and model scales, and $U_m(t_m)$ is termed the target speed. Note that this relationship must be satisfied throughout the entire time history of the maneuver. The Reynolds scale effect, which alters model scale resistance, requires that propeller RPM be adjusted to compensate and preserve this Froude-scaled speed relationship as discussed in the previous section. Note also that Eq. 43 is identical to Eq. 32, which is one of the two conditions to also satisfy the Strouhal number. The other condition, Eq. 31, will be addressed below in the section on angular velocity scaling.

Time Scaling

By definition,

$$a_s(t_s) = \frac{dU_s(t_s)}{dt_s}. \tag{44}$$

Integrating, we find that

$$\begin{aligned} \int dt_s &= \int \frac{1}{a_s}\, dU_s \\ t_s &= \int \frac{1}{a_m} \sqrt{\lambda}\, dU_m \quad \text{where } a_s = a_m \text{ and } \mathrm{d}U_s = \sqrt{\lambda}\, dU_m, \\ t_s &= \sqrt{\lambda}\, t_m \end{aligned} \tag{45}$$

and this represents the relationship between the time base to be used at full and model scales.

Linear Displacement Scaling

In a similar manner, we have, by definition,

$$U_s(t_s) = \frac{dx_s(t_s)}{dt_s}. \tag{46}$$

Integrating this expression, yields

$$\begin{aligned} \int dx_s &= \int U_s\, dt_s \\ x_s(t_s) &= \int \sqrt{\lambda}\, U_m \sqrt{\lambda}\, dt_m \quad \text{where } U_s = \sqrt{\lambda}\, U_m \text{ and } t_s = \sqrt{\lambda}\, t_m, \\ x_s(t_s) &= \lambda\, x_m(t_m) \end{aligned} \tag{47}$$

and relates the time history of ship trajectory at each scale.

Angular Acceleration Scaling

Recall from Eqs. 4,.

$$\left(\frac{(I_0+I_1)\frac{d^2\alpha}{dt^2}}{1/2\rho U^2 S L}\right)_m = \left(\frac{(I_0+I_1)\frac{d^2\alpha}{dt^2}}{1/2\rho U^2 S L}\right)_s . \tag{4}$$

As with added mass, we will assume that viscous effects associated with added moment of inertia are small, that is

$$\frac{[I_0+I_1]_m}{[I_0+I_1]_s} \approx \frac{[I_0]_m}{[I_0]_s} . \tag{48}$$

Moment of inertia I is defined by

$$I_x = \int x^2 dm \quad I_y = \int y^2 dm \quad I_z = \int z^2 dm . \tag{49}$$

We will make the assumption that the model can be fabricated to satisfy

$$\frac{[I_x]_m}{[I_x]_s} = \frac{[I_y]_m}{[I_y]_s} = \frac{[I_z]_m}{[I_z]_s} = \frac{\rho_s}{\rho_m}\lambda^5 . \tag{50}$$

In practice, to satisfy Eq. 50 is not an easy task. Information on full scale moment of inertia data will be required. Furthermore, obtaining a required mass distribution in the model may prove to be time consuming or impossible to achieve. A method to circumvent this possible fabrication difficulty is being investigated.

Substituting Eqs. 48 and 50 into Eq. 4 gives

$$\left[\frac{d^2\alpha}{dt^2}\right]_s = \frac{1}{\lambda}\left[\frac{d^2\alpha}{dt^2}\right]_m . \tag{51}$$

This equation states that the angular acceleration time history observed at full scale can be predicted from model angular acceleration data divided by the scale ratio $\lambda = L_s/L_m$.

Angular Velocity Scaling

The angular velocity is defined as

$$\frac{d\alpha}{dt} = \int \frac{d^2\alpha}{dt^2}\, dt\,. \tag{52}$$

Note that $dt_s = \sqrt{\lambda}\, dt_m$ is invariant in linear motion or in angular motion. Substitution of this and Eq. 51 into the above equation results in

$$\left[\frac{d\alpha}{dt}\right]_s = \frac{1}{\sqrt{\lambda}}\left[\frac{d\alpha}{dt}\right]_m. \tag{53}$$

This is an important result. One of the assumptions required for the Strouhal scale to be preserved during model testing is Eq. 31, which is repeated below.

$$\left[\frac{d\alpha}{dt}\right]_m = \left[\frac{d\alpha}{dt}\right]_s \frac{U_s}{U_m}. \tag{31}$$

Substituting Eq. 43 into Eq. 31 shows that it matches Eq. 53. Therefore, if these relationships obtained from Froude scaling are preserved throughout the maneuver, then the Strouhal scale will also be matched ensuring that unsteady effects are similar.

Angle Scaling

An angle results from integration of an angular velocity as follows

$$\alpha = \int \frac{d\alpha}{dt}\, dt\,. \tag{54}$$

Substitution of $dt_s = \sqrt{\lambda}\, dt_m$ and Eq. 53 into the above equation gives

$$\alpha_s(t_s) = \alpha_m(t_m)\,. \tag{55}$$

This is an important result. One of the assumptions required for restoring moment to be preserved in RCM tests is the second of Eqs. 27. This assumption is now verified by Eq. 55, where $\alpha_i = (\varphi, \theta, \psi)$ and φ, θ and ψ represent roll, pitch, and yaw angles, respectively.

Summary of Transfer Functions

The scaling formulas that relate model and full scale maneuvering behavior are summarized in Table 3. We are pleased to report that these formulas are used in the existing test procedure. We have systematically derived these formulas from first principles using the similarity scaling approach defined herein. The requirements needed to obtain Table 3 are clearly specified. A new test procedure is proposed so that these requirements are realized in RCM tests.

Table 3. Scaling Formulas

Quantity	Formula
Linear Acceleration	$a_s(t_s) = a_m(t_m)$
Linear Velocity	$U_s(t_s) = \sqrt{\lambda}\, U_m(t_m)$
Linear Displacement	$x_s(t_s) = \lambda\, x_m(t_m)$
Angular Acceleration	$\left[\frac{d^2\alpha}{dt^2}\right]_s = \frac{1}{\lambda}\left[\frac{d^2\alpha}{dt^2}\right]_m$
Angular Velocity	$\left[\frac{d\alpha}{dt}\right]_s = \frac{1}{\sqrt{\lambda}}\left[\frac{d\alpha}{dt}\right]_m$
Angle	$\alpha_s(t_s) = \alpha_m(t_m)$
Time	$t_s = \sqrt{\lambda}\, t_m$

Within the framework of the present mathematical formulation, we have shown that the Strouhal scale can be satisfied in RCM tests if the Froude scale is matched. Corrections have been introduced in order that Reynolds scale effects on forces and moments acting on the full scale craft are correctly simulated in model tests with the proviso that the assumptions introduced in Eqs. 48 and 50 hold. To compensate for the scale effect on ship resistance, propeller RPM can be adjusted to match the Froude-scaled target speed. Furthermore, as a result of relatively low Reynolds numbers on the model, and the location of appendages in a relatively thick model hull boundary layer, significant scale effects on forces and moments will be experienced by: rudders and sternplanes, the sail (moderate effect), and the ship hull (smaller effect). Methods to alleviate these effects on forces and moments have been proposed.

Concluding Remarks

We consider the modeling of maneuvering histories of ship motion, trajectory and attitude to be expressed by differential equations with terms that resemble a spring-mass system. Forces and moments acting on the vehicle and the subsequent ship motions in RCM tests and full scale trials are formulated based on a similarity approach. Within the framework of the present mathematical formulation, requirements and test methods to match Froude, Strouhal, and Reynolds scales (achieved dynamically) in RCM tests are discussed.

We postulate that: if the Strouhal scale can be preserved, then the unsteady forces and phase produced by the ship in response to the excitation forces and the subsequent unsteady motions will be correctly simulated. Studies reveal that the Strouhal scale can be satisfied in RCM tests if: (1) the Froude scale can be matched and (2) Reynolds scale effects on forces and moments acting on the craft can be correctly simulated and (3) restoring moments in pitch and roll motions can be correctly simulated.

The Froude scale *at each instant of the maneuver* can be satisfied by adjusting the propeller RPM. Experience must be gained to develop a workable procedure to tune the RPM time history.

As a result of relatively low Reynolds numbers on the model, and the location of appendages in a relatively thick model hull boundary layer, significant scale effects on forces and moments will be experienced by: rudders and sternplanes, the sail (moderate effect), and the ship hull (smaller effect). Methods to alleviate these effects on forces and moments have been proposed. During a tight turn maneuver, scale effects on flow separation will have to be investigated.

Scaling formulas have been derived from similarity solutions. We have assumed that

$$\frac{[I_x]_m}{[I_x]_s} = \frac{[I_y]_m}{[I_y]_s} = \frac{[I_z]_m}{[I_z]_s} = \frac{\rho_s}{\rho_m}\lambda^5 \tag{50}$$

is satisfied on RCM models. If not, the scaling formulas shown in Table 3 require modification. Finally, the assumption that added mass and moment of inertia are insensitive to Reynolds scale effects should be verified.

Acknowlegements

The U.S. Office of Naval Research sponsors this work through the Turbulence & Stratified Wakes Program. The program officer is Dr. Ronald Joslin, Code 331. Valuable technical comments and suggestions by Tom Moran, Kurt Junghans and Sam Cubbage are greatly appreciated. We would like to extend special thanks to Dr. Edward Ammeen for his continuous encouragement, guidance, discussion and support.

References

1. Baker, W.E., P.S. Westine and F.T. Dodge, Similarity Methods in Engineering Dynamics, Hayden Book Company, Inc., Rochelle Park, NJ, (1973).
2. Blake, W.K., "Aero-Hydroacoustics for Ships," DTNSRDC-84/010, (June 1984).
3. Bridges, D.H., J.N. Blanton, W.H. Brewer and J.T. Park, "Experimental Investigation of the Flow Past a Submarine at an Angle of Drift," AIAA Journal, (January 2003).
4. Faller, W.E. and C.F. Merrill, "ONR Body 1-Submarine Radio Controlled Model Experiments Part 1: Model Geometry," NSWCCD-50-2001/015, (April 2001).
5. Fu, T.C., A. Shekarriz, J. Katz, and T.T. Huang, "The Flow Structure in the Lee of an Inclined 6:1 Prolate Spheroid," Journal of Fluid Mechanics, 269, (1994).
6. Gukhman, A., Introduction to the Theory of Similarity, Academic Press, New York, (1965).
7. Han, T. and V. Patel, "Flow separation on a spheroid at incidence," Journal of Fluid Mechanics, 92, (1979).
8. Hess, D.E., T.C. Fu and J. P. Feldman, "Naval Maneuvering Research and the Need for Shear Stress Measurements," AIAA Paper 2004-2605, Portland, Oregon, (July 2004).
9. Hoang, N., T. Wetzel, and R. Simpson, "Surface Pressure Measurements over a 6:1 Prolate Spheroid Undergoing Time-Dependent Maneuvers," AIAA-94-1908-CP, (1994).
10. Howarth, L., "The Theoretical Determination of the Lift Coefficient for a Thin Elliptical Cylinder," Proc. Royal Society of London, Series A-Mathematical and Physical Sciences, 149, (April 1935).
11. Lewis, E.V., Principles of Naval Architecture, Second Revision, Society of Naval Architects and Marine Engineers, Jersey City, NJ, (1989).
12. Lloyd, A.R.J.M., Seakeeping – Ship Behaviour in Rough Weather, Ellis Horwood Limited, England, (1989).
13. Loftin, L.K. and W.J. Bursnall, "The Effect of Variations in Reynolds Number between $3.0x10^6$ and $25.0x10^6$ upon the Aerodynamic Characteristics of a Number of NACA 6-series Airfoil Sections," NACA Rep 964, (1950).
14. Loftin, L.K. and H.A. Smith, "Aerodynamic Characteristics of 15 NACA Airfoil Sections at Seven Reynolds Numbers from $0.7x10^6$ to $9.0x10^6$," NACA TN 1945, (Oct. 1949).
15. Schlichting, H., Boundary-Layer Theory, McGraw-Hill Book Company, (1979).
16. Shen, Y.T. and D. Fuhs, "Dynamic Effects on Propeller Blade Section Lift, Drag and Pitching Moment Coefficients," NSWCCD-50-1999/036, (August 1999).
17. Shen, Y.T. and M. Strasberg, "The Effect of Scale on Propeller Tip-Vortex Cavitation Noise," NSWCCD-50-TR-2003/057, (December 2003).
18. Spence, D.A., "Prediction of the Characteristics of Two-Dimensional Airfoils," Journal of Aeronautical Sciences, 21, (September 1954).

19. Szebehely, V.G., "Generalization of the Dimensionless Frequency Parameter in Unsteady Flows," DTMB Report 833, (November 1952).

20. Szebehely, V.G., "A Measure of Unsteadiness of Time-Dependent Flows," Third Midwestern Conference on Fluid Mechanics, (March 1953).

21. Theodorsen, T., "General Theory of Aerodynamic Instability and the Mechanism of Flutter," NACA Report 496, (1935).

22. Whicker L.F. and L.F. Fehlner, "Free-Stream Characteristics of a Family of Low-Aspect-Ratio, All-Movable Control Surfaces for Application to Ship Design," DTMB Report 933, (December 1958).

INITIAL DISTRIBUTION

Copies	Organization	Code	Letter Only	Paper Copy	PDF	Name
1	DTIC			Y		
1	NAVSEA	PMS394			Y	T. Cary
1	NAVSEA	05H			Y	M. King
1	ONR	331		Y		R. Joslin
1	NSWCCD	3452			Y	TIC(C)
1	NSWCCD	5060		Y		D. Walden
1	NSWCCD	5080			Y	J. Brown
1	NSWCCD	5080	Y			B. Cox
1	NSWCCD	5400			Y	J. Gorski
1	NSWCCD	5600			Y	E. Ammeen
1	NSWCCD	5600	Y		Y	S. Cubbage
1	NSWCCD	5600	Y		Y	K. Junghans

THIS PAGE INTENTIONALLY LEFT BLANK